The Mass Ratio Distribution of Black Hole Mergers Induced by a Comparable Mass Tertiary

Accepted XXX. Received YYY; in original form ZZZ

ABSTRACT

Abstract

Key words: binaries:close – stars:black holes

1 INTRODUCTION

We study the von Zeipel-Lidov-Kozai effect (ZLK) for eccentric perturbers to octupole order, also sometimes known as the eccentric Kozai mechanism (e.g. Lithwick & Naoz 2011).

The mass ratio distribution among ZLK-induced BBH mergers has already been noted (see Fig. 10 of Silsbee & Tremaine 2017), but the origin of the effect has not been carefully studied.

2 DYNAMICS WITHOUT GRAVITATIONAL WAVE RADIATION

We first briefly review results in regimes of increasing complexity.

We use the octupole-order, double-averaged vectorial ZLK equations from LML15 (Liu et al. 2015), including 1PN de Sitter apsidal precession. In this section, we neglect 2.5PN GW radiation (Peters 1964), but will consider it later in Section 3.

2.1 Quadrupole-Order ZLK

When considering the EOM to quadrupole order, the eccentricity of the inner binary cycles regularly over $\sim t_{\rm ZLK}$ with

$$t_{\rm LK} = \frac{1}{n_1}\frac{m_{12}}{m_3}\left(\frac{a_{\rm out,eff}}{a}\right)^3, \tag{1}$$

where $a_{\rm out,eff} \equiv a_{\rm out}\sqrt{1-e_{\rm out}^2}$. Our fiducial parameters are: $a = 100$ AU, $a_{\rm out,eff} = 3600$ AU, $m_{12} = 50M_\odot$, $m_3 = 30M_\odot$.

The dynamics to quadrupole order depend on the ratio of the angular momenta, given by

$$\eta \equiv \left.\frac{L}{L_{\rm out}}\right|_{e=0} = \frac{\mu}{\mu_{\rm out}}\left[\frac{m_{12}a}{m_{123}a_{\rm out}\left(1-e_{\rm out}^2\right)}\right]^{1/2}. \tag{2}$$

Note that to quadrupolar order, $e_{\rm out}$ and thus η are constant.

We further have the following results:

- The system spends a fraction $\sim j(e_{\rm max})$ of each ZLK eccentricity cycle near $e_{\rm max}$ (Anderson et al. 2016).
- Two conserved quantities, energy and $K \equiv j\cos I - \eta e^2/2$. It is the general conserved quantity which when $\eta = 0$ reduces to the classical "Kozai Constant" (Liu et al. 2015).

When 1PN is considered, the strength is measured by

$$\epsilon_{\rm GR} \equiv \frac{3Gm_{12}}{c^2}\frac{m_{12}}{m_3}\frac{a_{\rm out,eff}^3}{a^4}. \tag{3}$$

This gives further results:

- It can be shown that $e_{\rm max}$ and $j_{\rm min} \equiv j(e_{\rm max})$ for a given I_0 obeys (Liu et al. 2015; Anderson et al. 2016):

$$\frac{3}{8}\frac{j_{\rm min}^2-1}{j_{\rm min}^2}\left[5\left(\cos I_0+\frac{\eta}{2}\right)^2-\left(3+4\eta\cos I_0+\frac{9}{4}\eta^2\right)j_{\rm min}^2 + \eta^2 j_{\rm min}^4\right]+\epsilon_{\rm GR}\left(1-1/j_{\rm min}\right)=0. \tag{4}$$

The minimum value of $j_{\rm min}$, denoted $j_{\rm lim}$, occurs when $I_0 = I_{0,\rm lim}$, where

$$\cos I_{0,\rm lim} = \frac{\eta}{2}\left(\frac{4}{5}j_{\rm lim}^2-1\right). \tag{5}$$

Note that $I_{0,\rm lim} \geq 90^\circ$ with equality only when $\eta = 0$. Substituting Eq. (5) into Eq. (4) gives

$$\frac{3}{8}\left(j_{\rm lim}^2-1\right)\left[-3+\frac{\eta^2}{4}\left(\frac{4}{5}j_{\rm lim}^2-1\right)\right]+\epsilon_{\rm GR}\left(1-1/j_{\rm lim}\right)=0. \tag{6}$$

2.2 Octupole-Order ZLK, Test-Particle Limit

Well-studied in test particle limit where $m_2 = 0$ and $\eta = 0$, we review a few relevant results. In this limit, define

$$\epsilon_{\rm oct}^{\rm (tp)} = \frac{a}{a_{\rm out}}\frac{e_{\rm out}}{1-e_{\rm out}^2}. \tag{7}$$

- In this limit, $K = j\cos I$.
- When $0 < \epsilon_{\rm oct}$, orbit flips become possible, and during these orbit flips, $e = e_{\rm lim}$ is attained (Lithwick & Naoz 2011; Liu et al. 2015). The range of inclinations for which this is possible is wider than the quadrupole-only case.
- Katz et al. (2011) show that, with $0 < \epsilon_{\rm oct} \ll 1$, K oscillates in a well-behaved way. An approximate analytic calculation gives an accurate prediction of this orbit-flipping window when $\epsilon_{\rm oct} \ll 1$ and when ω, the argument of pericenter of the inner orbit, is circulating. Timescale is given by Antognini (2015).

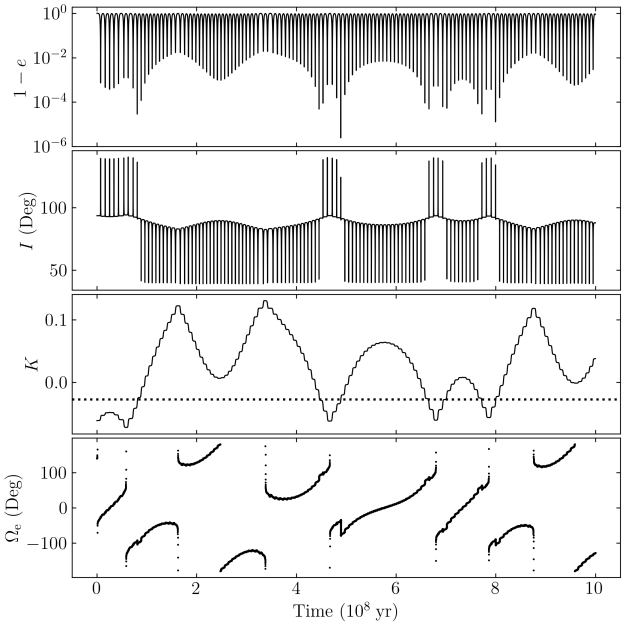

Figure 1. Fiducial simulation showing orbit flips, which occur when K crosses the dotted line $K = K_c \approx \eta/2$. $I_0 = 93.5°$. When ω is circulating, the angle Ω_e (the co-longitude of the inner eccentricity vector) changes slowly (Katz et al. 2011).

- (Muñoz et al. 2016) shows that the octupole-active region can be well fit by a fitting formula for $\epsilon_{\rm oct}$ as large as 0.07. The blue dots in top panel of Fig. 2 show that indeed the maximum eccentricity reaches $e_{\rm lim}$ within this inclination range.

2.3 Octupole-Order ZLK, General Masses

When m_1, m_2 are comparable, Eq. (7) generalizes to

$$\epsilon_{\rm oct} = \frac{m_1 - m_2}{m_{12}} \frac{a}{a_{\rm out}} \frac{e_{\rm out}}{1-e_{\rm out}^2}. \tag{8}$$

The comparable-mass regime is qualitatively different from the test-particle regime (e.g. Rodet et al, 2021). We show a fiducial simulation in Fig. 1

- No analytic solution to predict amplitude of K (generalized version) oscillations, though qualitative behavior is the same.
- Asymmetric octupole-active region (see top panels of Figs. 3–5).
- We describe the behavior with two characteristic eccentricities: $e_{\rm max}$ and an effective $e_{\rm eff}$. The latter is defined via an average over many ZLK cycles (denoted by angle brackets) and $j_{\rm eff} \equiv \sqrt{1-e_{\rm eff}^2}$:

$$\left\langle \frac{{\rm d}\ln a}{{\rm d}t} \right\rangle \approx -\frac{1}{t_{\rm GW,0}} \left\langle \frac{1 + 73e_{\rm max}^2/24 + 37e_{\rm max}^4/96}{j_{\rm min}^6} \right\rangle \equiv -\frac{421/96}{t_{\rm GW,0}} \frac{1}{j_{\rm eff}^6}. \tag{9}$$

3 WITH GW

We turn on GW, binaries will either merge or not within 10 Gyr, produces middle panels of Fig. 3.

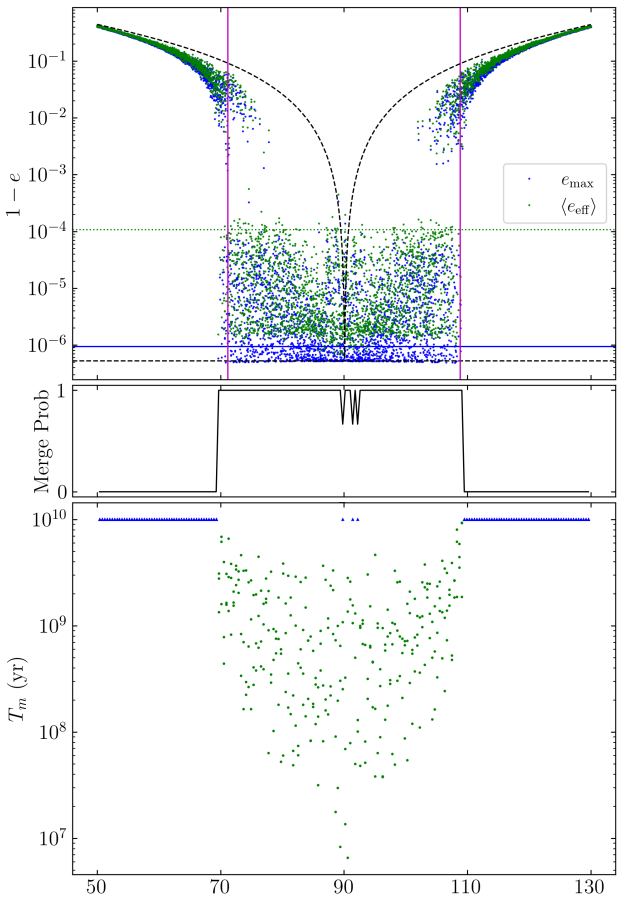

Figure 2. Fiducial parameters but for $q = 0.01$, i.e. in the test-particle regime $\eta \ll 1$. The purple vertical lines are the fitting formula of Muñoz et al. (2016) and are accurate. TODO Explore the merging window more densely.

- Define $e_{\rm os}$, and $j_{\rm os} = \sqrt{1-e_{\rm os}^2}$, the $e_{\rm max}$ required to produce a one-shot merger ZLK:

$$j\,(e_{\rm os})\,\frac{{\rm d}\ln a}{{\rm d}t}\bigg|_{e=e_{\rm os}} \sim \frac{1}{t_{\rm ZLK}}, \tag{10}$$

$$j_{\rm os}^6 = \frac{256}{5}\frac{G^3\mu m_{12}^3}{m_3 c^5 a^4 n}\left(\frac{a_{\rm out,eff}}{a}\right)^3. \tag{11}$$

If an IC has $e_{\rm max} \gtrsim e_{\rm os}$, then gives one-shot merger. See comparison between top and middle panels for Figs. 2–5.

- Define $e_{\rm eff,c}$ and $j_{\rm eff,c} \equiv \sqrt{1-e_{\rm eff,c}^2}$, the critical effective eccentricity, such that

$$\left\langle \frac{{\rm d}\ln a}{{\rm d}t} \right\rangle = \frac{421/96}{t_{\rm GW,0} j_{\rm eff,c}^6} = 10\ {\rm Gyr}. \tag{12}$$

If an IC has $e_{\rm eff} \gtrsim e_{\rm eff,c}$, then gives gradual merger.

For wide binaries, systems generally satisfy $e_{\rm max} \gtrsim e_{\rm os}$ if and only if they satisfy $e_{\rm eff} \gtrsim e_{\rm eff,c}$. However, this need not be the case, see Fig. 6.

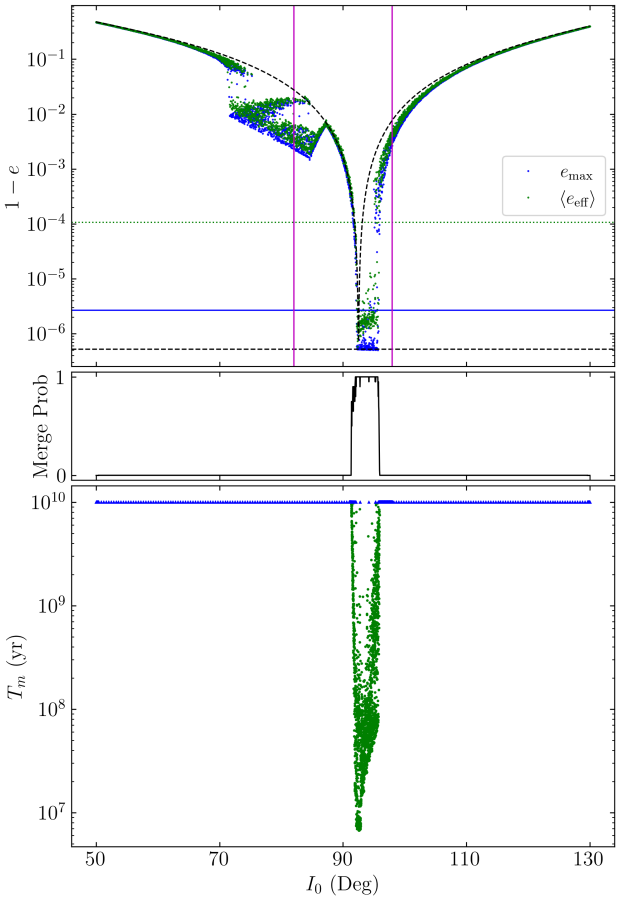

Figure 3. Same as Fig. 2 but where $q = 0.5$.

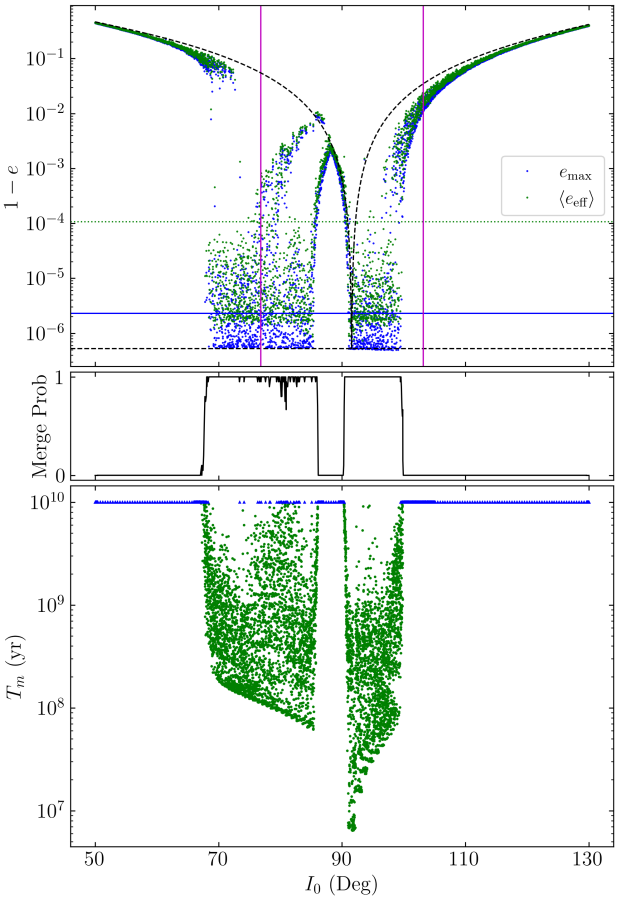

Figure 4. Same as Fig. 3 but for $q = 0.2$.

4 MASS RATIO SIGNATURE IN A POPULATION OF MERGING BBHS

A physically representative ensemble is beyond the scope of this paper, and we instead focus on simple, illustrative populations of BBH to demonstrate the effect.

4.1 Fixed Tertiary Eccentricity

We first consider the simplified case where the tertiary eccentricity is fixed, and seek the merger probability as a function of mass ratio q. For these, we let $\cos I_0$ be drawn uniformly from the range $[-1, 1]$, and fix everything else. See Fig. 7. This suggests that low mass ratio mergers should be more common.

- For sufficiently small $\epsilon_{\rm oct}$, the merger probability does not depend on $e_{\rm out}$ and q separately but only on their combination via $\epsilon_{\rm oct}$.
- However, when $\epsilon_{\rm oct}$ is sufficiently large, an $e_{\rm out}$ dependence is introduced. This is because the size of the gap (see e.g. Fig. 5), and the value of $\epsilon_{\rm oct}$ when prograde systems are able to merge, depend on q through η. A discussion of this gap is in Appendix A.

We also examine what happens when $a = 50$ AU; This figure is still being generated.

4.2 Distribution of Tertiary Eccentricities

We can also draw $e_{\rm out} \in [0, 0.9]$. We try either uniform probability or thermal $P(e_{\rm out}) \propto e_{\rm out}$. The results are given for our fiducial $a_{\rm out,eff} = 3600$ AU in Fig. 8. For comparison, we also show the results when $a_{\rm out,eff} = 5500$ AU.

- Note: LIGO-band eccentricities are small, but nonetheless show a small q dependence, which may be detectable in the LISA band.

4.3 Effect of Smaller Mass Ratios

Intuitively, $q \to 0$ means $t_{\rm GW,0} \to \infty$ and no mergers. This would predict more large-mass-ratio mergers, opposite to our observed trend. Why is this?

When orbital flips occur, $e_{\max}$ attains $e_{\rm lim}$. This induces one-shot mergers when $e_{\rm lim} > e_{\rm os}$, or when

$$\left(\frac{a}{a_{\rm out,eff}}\right) \gtrsim 0.0118 \left(\frac{a_{\rm out,eff}}{3600\ {\rm AU}}\right)^{-7/37} \left(\frac{m_{12}}{50M_\odot}\right)^{17/37} \times \left(\frac{30M_\odot}{m_3}\right)^{10/37} \left(\frac{q/(1+q)^2}{1/4}\right)^{-2/37}. \quad (13)$$

This shows that q must be changed by many orders of magnitude to transition between a parameter regime where one-shot mergers occur at orbital flips to one where such mergers fail to occur.

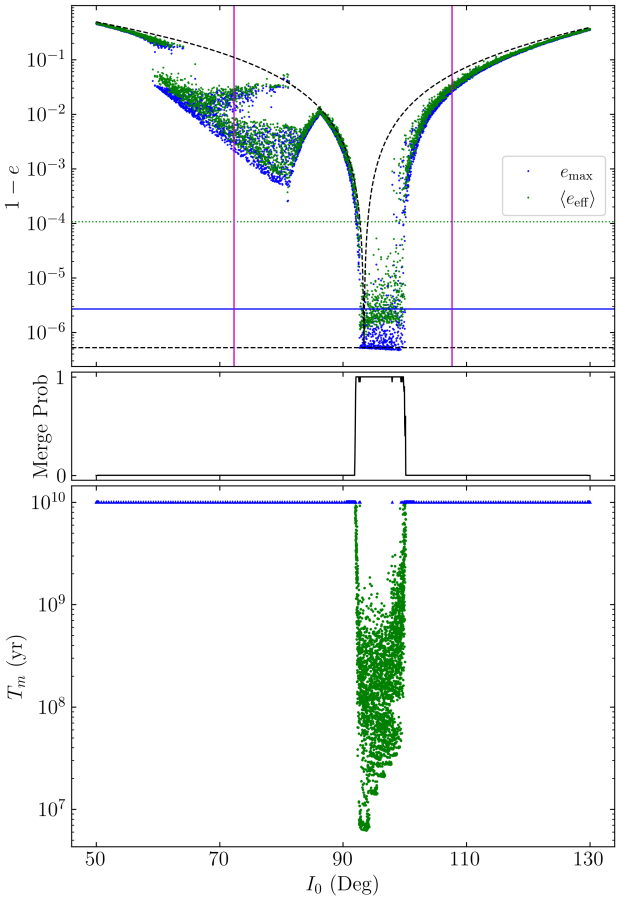

Figure 5. Same as Fig. 3 but $e_{\rm out} = 0.9$ while holding $a_{\rm out,eff} = 3600$ AU constant.

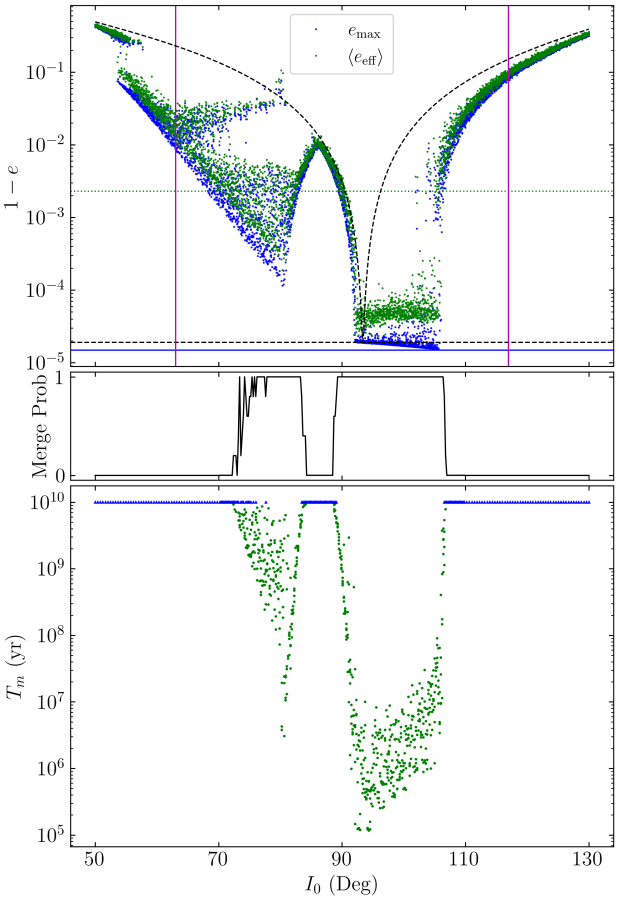

Figure 6. Same as Figs. 2–4 but for a compact inner binary, 10 AU. Note that $e_{\max} < e_{\rm os}$ but $e_{\rm eff} > e_{\rm eff,c}$ for the merging systems that are prograde ($I_0 < 90°$).

5 CONCLUSION

- Primordial q distribution in massive stellar binaries: tends to be skewed towards smaller q to varying degrees (Sana et al. 2012; El-Badry et al. 2019).
- Eccentricity distribution of tertiary? Likely to be between uniform and thermal.
- LIGO O3a bounds on the BBH q distribution: if $P(q) = q^{\beta_q}$, then $\beta_q > 0$ at 89% or more, depending on the model (Abbott et al. 2020), implying favoring equal-mass binaries.
- Our parameters are not particularly fine-tuned. If the inner binary is tighter or the perturber farther, then the MLL16 fits are better and give the same qualitative result. If the inner binary is looser, flybys become important. If the perturber is closer, then DA breaks down.

6 ACKNOWLEDGEMENTS

YS is supported by the NASA FINESST grant 19-ASTRO19-0041.

REFERENCES

Abbott R., et al., 2020, arXiv preprint arXiv:2010.14533
Anderson K. R., Storch N. I., Lai D., 2016, Monthly Notices of the Royal Astronomical Society, 456, 3671
Antognini J. M., 2015, Monthly Notices of the Royal Astronomical Society, 452, 3610
El-Badry K., Rix H.-W., Tian H., Duchêne G., Moe M., 2019, Monthly Notices of the Royal Astronomical Society, 489, 5822
Katz B., Dong S., Malhotra R., 2011, Physical Review Letters, 107, 181101
Lithwick Y., Naoz S., 2011, The Astrophysical Journal, 742, 94
Liu B., Muñoz D. J., Lai D., 2015, Monthly Notices of the Royal Astronomical Society, 447, 747
Muñoz D. J., Lai D., Liu B., 2016, Monthly Notices of the Royal Astronomical Society, 460, 1086
Peters P. C., 1964, Physical Review, 136, B1224
Sana H., et al., 2012, Science, 337, 444
Silsbee K., Tremaine S., 2017, The Astrophysical Journal, 836, 39

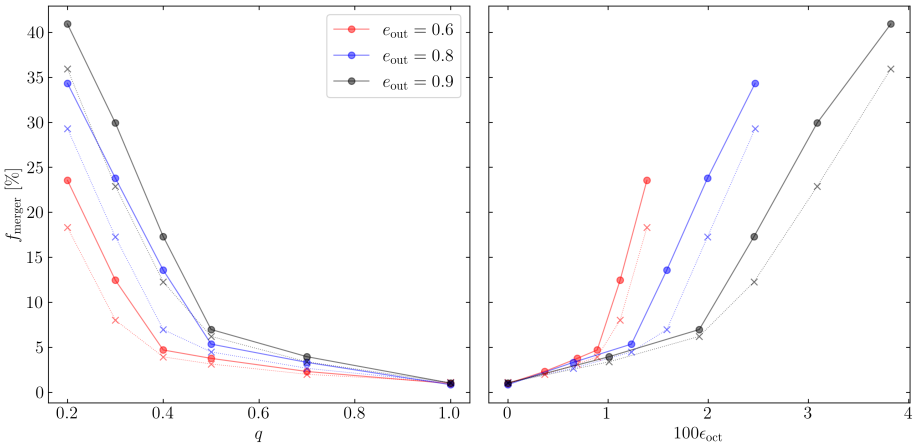

Figure 7. Merger probability for fixed tertiary eccentricity as a function of mass ratio, fiducial params. Dotted lines represent the prediction using the GW-free criteria.

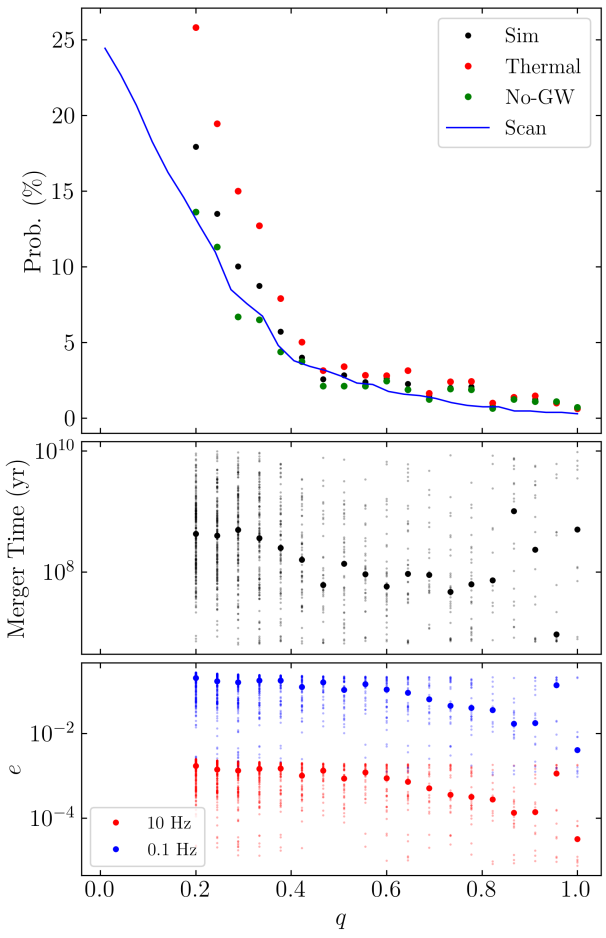

Figure 8. When $e_{\rm out}$ is drawn from a distribution too. Big dots in bottom two panels are medians.

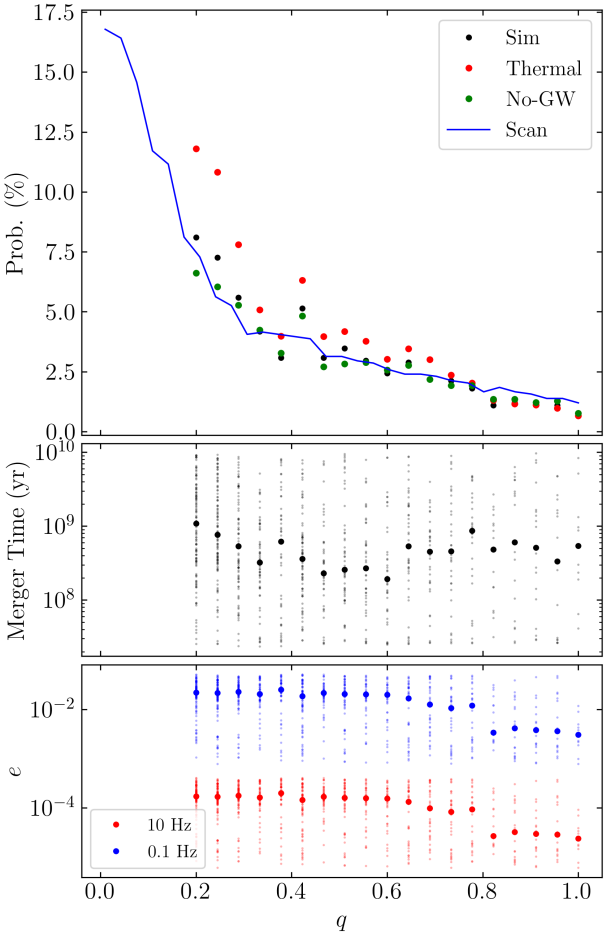

Figure 9. Same as Fig. 8 but for $a_{\rm out,eff}$ = 5500 AU.

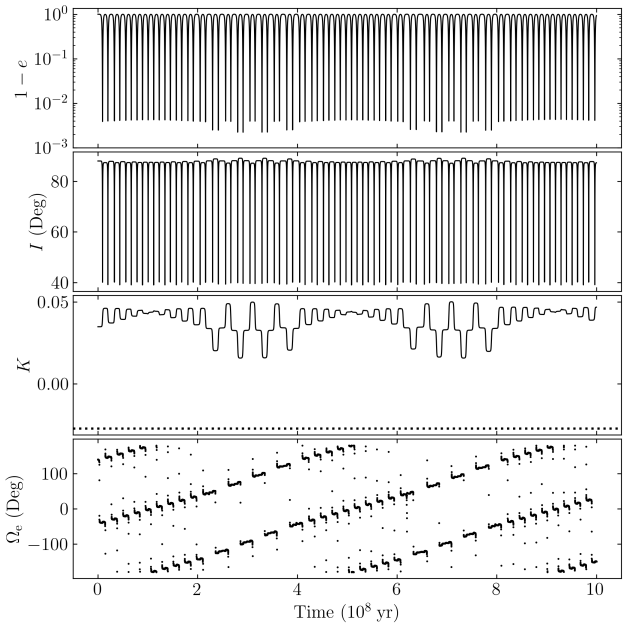

Figure A1. Example simulation where Ω_e is primarily circulating, which suppresses the amplitude of oscillation of K. As a result, the orbit does not flip.

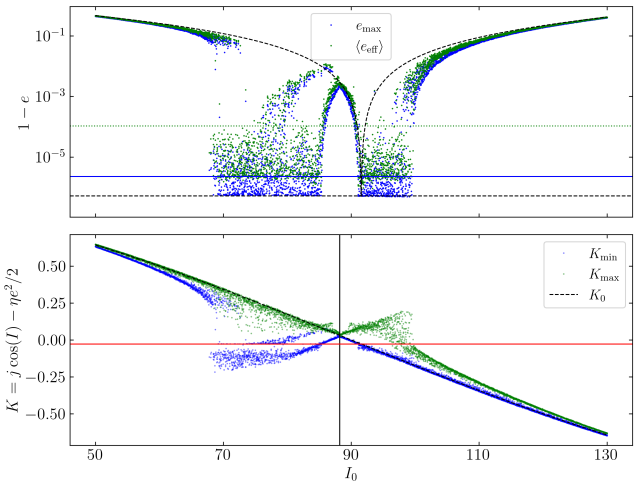

Figure A2. $K_{\min}$ and $K_{\max}$ range of oscillation for the same parameters as Fig. 4.

APPENDIX A: ORIGIN OF OCTUPOLE-INACTIVE GAP

- Example simulation where librating, Fig. A1.
- Show the $K_{\min}$ and $K_{\max}$ plot, Fig. A2.
- Point out that librating solutions are the origin of the gap, Fig. A3.

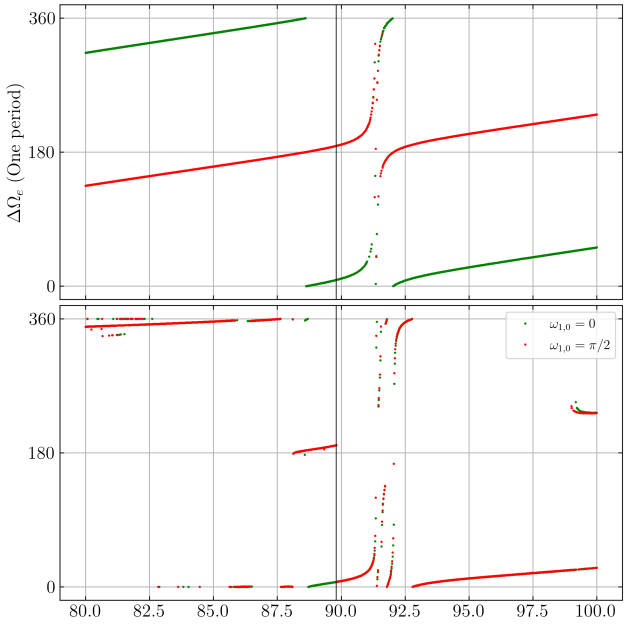

Figure A3. When octupole terms are off (top), circulating and librating ω_0 have the right $\Delta\Omega_e$, but when octupole terms are on (bottom), the transition instead does not depend on ω_0 but I_0.